PHASE TRANSITIONS IN MEMBRANES

Abdel K. Tahari

April, 30, 2000

Abstract

The fluctuations of two-dimensional extended objects (membranes) is a rich and exciting field with many solid results and a wide range of open issues. In this term paper we review the distinct universality classes of membranes, determined by the local order, and the associated phase diagrams. After a discussion of several physical examples of membranes we turn to the physics of crystalline (or polymerized) membranes in which the individual monomers are rigidly bound. We discuss the phase diagram with particular attention to the dependence on the degree of self-avoidance and anisotropy. The resulting renormalization group flows and fixed points are illustrated graphically. We then turn to a brief discussion of the role of topological defects whose liberation leads to the hexatic and fluid universality classes. We finish with conclusions and a discussion of promising open directions for the future.

1 Introduction

The subject of two-dimensional extended objects (membranes) is a fascinating field of research. The statistical mechanics of these random surfaces is far more complex than that of polymers because two-dimensional geometry is far richer than the very restricted geometry of lines. Membranes are subject to shape fluctuations and their macroscopic behavior is determined by a subtle interplay between their particular microscopic order and entropy of shape and elastic deformations. For membranes, unlike polymers, distinct types of microscopic order (crystalline, hexatic, fluid) will lead to distinct long-wavelength behavior and consequently a rich set of universality classes.

Flexible membranes are an important member of the enormous class of soft condensed matter systems, those which respond easily to external forces. Their physical properties are to a considerable extent dominated by the entropy of thermal fluctuations.

2 Physical Examples of Membranes

Many concrete realizations of membranes exist in nature. Crystalline membranes, also called tethered or polymerized membranes, possess in-plane elastic moduli as well as bending rigidity and are characterized by broken translational invariance in the plane and fixed connectivity due to relatively strong bonding. The cytoskeletons of cell membranes are beautiful and naturally occurring crystalline membranes that are essential to cell membrane stability and functionality. The simplest and thoroughly studied example is the cystoskeleton of mammalian red blood cells (erythrocytes). They are a fishnet-like network of triangular plaquettes formed primarily by the proteins spectrin and actin. The links of the mesh are spectrin tetramers approximately 200nm-long and the nodes are short actin filaments typically 37nm-long. There are roughly 70,000 plaquettes in the mesh. There are also inorganic realizations of crystalline membranes. Graphitic oxide membranes are micron size sheets of solid carbon with thickness on the order of 10Å, forms by exfoliating carbon with a strong oxidizing agent. Metal dichalcogenides such as MoS_2 have also been observed to form rag-like sheets. Similar structures also occur in large sheet molecules, believed to be an ingredient in glassy B_2O_3.

In contrast to crystalline membranes, fluid membranes are characterized by vanishing shear modulus and dynamic connectivity. They exhibit significant shape fluctuations controlled by an effective bending rigidity parameter. A rich realization of these is found in amphiphilic systems. Amphiphiles are molecules with a two-fold character - one is hydrophobic and the other hydrophilic. The classical example is lipid molecules, such as phospholipids, which have polar or ionic head groups (hydrophilic) and hydrocarbon tails (hydrophobic). Such systems are observed to self-assemble into an array of ordered structures, such as monolayers, planar and spherical bilayers (vesicles and liposomes) as well as lamellar, hexagonal and

bicontinuous phases. In each case the basic ingredients are thin and highly flexible surfaces of amphiphiles. Related examples of fluid membranes arise when the surface tension between two normally immiscible substances, such as oil and water is significantly lowered by the surface action of surfactants, which preferentially orient with their polar heads in water and their hydrocarbon tails in oil. For some range of amphiphile concentration both phases can span the system, leading to a bicontinuous complex fluid known as a microemulsion.
The structures formed by membrane/polymer complexes are of considerable current theoretical, experimental and medical interest. It has recently been found that mixtures of cationic liposomes and linear DNA chains spontaneously self-assemble into a coupled two-dimensional smectic phase of DNA chains embedded between lamellar lipid bilayers. For the appropriate regime of lipid concentration the same system can also form an inverted hexagonal phase with DNA encapsulated by cylindrical columns of liposomes. In both cases the liposomes may act as non-viral carriers for DNA with many potentially important applications in gene therapy. Liposomes themselves have been studied and utilized in the pharmaceutical industry as drug carriers. On the materials science side the self-assembling ability of membranes is being exploited to fabricate microstructures for advanced material development. One example is the use of chiral-lipid based fluid tubules as a template for metallization. The resultant hollow metal needles may be half a micron in diameter and a millimeter in length. They have potential applications as, for example, cathodes for vacuum field emission and microvials for controlled release.

3 Crystalline Membranes

A crystalline membrane is a two-dimensional fishnet structure with non-breaking bonds (links). For the moment let's keep the discussion general and consider a D-dimensional object embedded in d-dimensional space. These are described by a d-dimensional vector $\vec{r}(x)$, with x the D-dimensional internal coordinates, as illustrated in Fig.1. The case $d = 3$ and $D = 2$ corresponds to the physical crystalline membrane.
To construct the Landau free energy, one must recall that it must be invariant under global translations, so the order parameter is given by derivatives of the embedding $\vec{r}$, that is $\vec{t}_\alpha = \frac{\partial \vec{r}}{\partial u_\alpha}$, with $\alpha = 1, \cdots, D$. This latter condition, together with the invariance under rotations, both in internal and bulk space, give a Landau free energy

$$F(\vec{r}) = \int d^D x [\frac{1}{2}\kappa(\partial_\alpha^2 \vec{r})^2 + \frac{t}{2}(\partial_\alpha \vec{r})^2 + u(\partial_\alpha \vec{r}\partial_\beta \vec{r})^2 + v(\partial_\alpha \vec{r}\partial^\alpha \vec{r})^2] + \frac{b}{2}\int d^D x d^D y \delta^d(\vec{r}(x) - \vec{r}(y)), \tag{1}$$

where higher order terms may be shown to be irrelevant at long wavelength.
The physics in eq.(1) depends on five parameters,

κ , bending rigidity: This is the coupling to the extrinsic curvature (the square

of the Gaussian mean curvature). This term may be replaced by its long-wavelength limit. For large and positive bending rigidities flatter surfaces are favored.

t, u, v, elastic constants: These coefficients encode the microscopic elastic properties of the membrane.

b, excluded volume or self-avoiding coupling: This is the coupling that imposes an energy penalty for the membrane to self-intersect. The case $b = 0$, no self-avoidance, corresponds to the Phantom model.

$\vec{r}(x)$ is generally expanded as

$$\vec{r}(x) = (\zeta x + u(x), h(x)), \tag{2}$$

with u the D-dimensional phonon in-plane modes, and h the $d - D$ out-of-phase fluctuations. If $\zeta = 0$ the model is in a rotationally invariant crumpled phase, where the typical surfaces have fractal dimension, and there is no real distinction between the in-plane phonons and the out-of-plane modes. If $\zeta \neq 0$ the membrane is flat up to small fluctuations and the full rotational symmetry is spontaneously broken.

We will begin by studying the phantom case first. This simplified model may be viewed as a first step toward the understanding of the more physical self-avoiding case to be discussed later. Combined analytical and numerical studies have yielded a thorough understanding of the phase diagram of phantom crystalline membranes.

3.1 Phantom model

The phantom case corresponds to setting $b = 0$ in the free energy of eq.(1)

$$F(\vec{r}) = \int d^D x [\frac{1}{2}\kappa(\partial_\alpha^2 \vec{r})^2 + \frac{t}{2}(\partial_\alpha \vec{r})^2 + u(\partial_\alpha \vec{r}\partial_\beta \vec{r})^2 + v(\partial_\alpha \vec{r}\partial^\alpha \vec{r})^2]. \tag{3}$$

The mean field effective potential using, eq. (2), becomes

$$V(\zeta) = D\zeta^2(\frac{t}{2} + (u + vD)\zeta^2), \tag{4}$$

with solutions

$$\zeta^2 = \begin{cases} 0 & : \quad t \geq 0 \\ -\frac{t}{4(u+vD)} & : \quad t < 0 \end{cases} \tag{5}$$

.

There is therefore a flat phase for $t < 0$ and a crumpled phase for $t > 0$, separated by a crumpling transition at $t = 0$. See Fig.2.

The phase diagram of the model is shown schematically in Fig.3. The crumpled phase is described by a line of equivalent FPs (GFP). There is a general hyper-surface, whose projection onto the $\kappa - t$ plane corresponds to a one-dimensional curve (CTH), which corresponds to the crumpling transition. Within the CTH there is an infrared stable FP (CTFP) which describes the large distance properties

of the crumpling transition. For large enough values of κ and negative values of t, the system is in a flat phase described by the corresponding infrared stable FP (FLFP). The evidence for the phase diagram comes from combining the results of a variety of analytical and numerical calculations.

3.1.1 The crumpled phase

In the crumpled phase, the free energy for $D \geq 2$ simplifies to

$$F(\vec{r}) = \frac{t}{2} \int d^D x (\partial_\alpha \vec{r})^2 + \text{Irrelevant terms} \tag{6}$$

All derivative operators in $\vec{r}$ are irrelevant by power counting since the model is completely equivalent to a linear sigma model in $D \leq 2$ dimensions having $O(d)$ symmetry. The parameter t labels different Gaussian FPs. In RG language, it defines a completely marginal direction. This is true provided that $t > 0$ is satisfied. The Hausdorff dimension d_H, or equivalently the size exponent $\nu = D/d_H$, is given for the membrane case $D = 2$ by

$$dH = \infty (\nu = 0) \rightarrow R_G^2 \sim \log L. \tag{7}$$

This result is in complete agreement with numerical simulations of tethered membranes in the crumpled phase where logarithmic behavior of the radius of gyration is accurately checked.

3.1.2 The crumpling transition

Different estimates give a continuous crumpling transition with a size exponent in the range $\nu \sim 0.7 \pm .15$. Further evidence of this is also provided by numerical simulations where the analysis of observables like the specific heat or the radius of gyration give textbook continuous phase transitions, although the precise value of the exponents at transition are difficult to pin down. Since this model has also been explored numerically with different discretizations on several lattices, there is clear evidence for universality of the crumpling transition.

3.1.3 The flat phase

In terms of the strain tensor

$$u_{\alpha\beta} = \partial_\alpha u_\beta + \partial_\beta u_\alpha + \partial_\alpha h \partial_\beta h \tag{8}$$

the free energy becomes

$$F(u,h) = \int d^D x [\frac{\hat{\kappa}}{2} (\partial_\alpha \partial_\beta h)^2 + \mu u_{\alpha\beta} u^{\alpha\beta} + \frac{\lambda}{2} (u_\alpha^\alpha)^2], \tag{9}$$

where irrelevant terms have been dropped.
As apparent from Fig.4, there are three FPs in addition to the FLFP already

introduced. These turn out to be infrared unstable and can be reached for very specific values of the coefficients. In this phase, the membrane is essentially a flat two-dimensional object up to fluctuations in the perpendicular direction. The rotational symmetry is spontaneously broken, being reduced from $O(d)$ to $O(d-D)\mathrm{x}O(D)$. Let's study the critical exponents of the model. There are two correlators involving the in-plane and the out-of-plane photon modes. Using the RG equations, at any given FP, the low-p limit of the model is given by

$$\Gamma_{uu}(\vec{p} \sim |\vec{p}|^{2+\eta_u} \tag{10}$$
$$\Gamma_{hh} = |\vec{p}|^4 \kappa(\vec{p}) \sim |\vec{p}|^{4-\eta}$$

where the last equation defines the anomalous elasticity $\kappa(\vec{p})$ as a function of momentum $\vec{p}$. These two exponents are not independent, since they satisfy the scaling relation

$$\eta_u = 4 - D - 2\eta. \tag{11}$$

Another exponent is the roughness exponent ζ which measures the transverse fluctuations. It can be expressed as $\zeta = (4 - D - \eta)/2$. The long wavelength properties of the flat phase are described by the FLFP. Results obtained from large-scale simulations of the model using very large meshes give

$$\eta_u = 0.50(1) \quad \eta = 0.750(5) \quad \zeta = 0.64(2) \tag{12}$$

There are two experimental measurements of critical exponents for the flat phase of crystalline membranes. The static structure factor of the red blood cell cystoskeleton has been measured by small-angle x-ray and light scattering, yielding a roughness exponent of $\zeta = 0.65(10)$. Freeze-fracture electron microscopy and static light scattering of the conformations of graphitic oxide sheets revealed flat sheets with a fractal dimension $d_H = 2.15(6)$. Both these values are in good agreement with the best analytic and numerical predictions. Finally another critical regime of the flat membrane is achieved by subjecting the membrane to external tension. This allows a low temperature phase in which the membrane has a domain structure, with distinct domains corresponding to flat phases with different bulk orientations. This describes physically a buckled membrane whose equilibrium shape is no longer planar.

3.2 Self-avoiding model

It is necessary to include self-avoidance interaction in any realistic description of a crystal membrane. It is usually introduced as a delta-function repulsion in the full model eq.(1). The question before us is the effect of self-avoidance on each of the different phases. The first phase we analyze is the flat phase. Since self-interactions are unlikely in this phase, it is intuitively clear that self-avoidance is irrelevant in the

flat phase. This argument receives additional support from numerical simulations, where it is found that self-avoidance is extremely rare in the flat phase. It seems clear that self-avoidance is most likely an irrelevant operator, in the RG sense, of the FLFP.
The addition of self-avoidance in the crumpled phase consists of adding the self-avoiding interaction to the free energy

$$F(\vec{r}) = \frac{1}{2}\int d^D x (\partial_\alpha^2 \vec{r})^2 + \frac{b}{2}\int d^D x d^D y \delta^d(\vec{r}(x) - \vec{r}(y)), \tag{13}$$

Standard power counting shows that the GFP of the crumpled phase is infra-red unstable to the self-avoiding perturbation for

$$\epsilon(D,d) = 2D - d\frac{2-D}{2} > 0, \tag{14}$$

which implies that self-avoidance is a relevant perturbation for $D = 2$ objects at any embedding dimension d. The preceding results are shown in Fig.5.
In summary, the flat phase of self-avoiding crystalline membrane is exactly the same as the flat phase of phantom crystalline tethered membranes. The crumpled phase of crystalline membranes is destabilized by the presence of any amount of self-avoidance.
The next issue we need to elucidate is whether this new SAFP describes a crumpled self-avoiding phase or a flat phase and discuss more quantitatively the critical exponents describing the universality class.

3.2.1 The nature and properties of the SAFP

The key issue is whether this model still admits a crumpled phase, and if so to determine the associated size exponent. On general grounds we expect that there is a critical dimension dc, below which there is no crumpled phase. Within a Flory approximation, a D-dimensional membrane is in a crumpled phase, with a size exponent given by $\nu = (D+2) = (d+2)$. From this it follows that $d_c = D$. In contrast, an ϵ-expansion provides a systematic determination of the critical exponents. At lowest order in ϵ, the membrane is in a crumpled phase. Some authors argue in favor of a scenario with a critical dimension $d_c \sim 4$. Within a Gaussian approximation, $\nu = 4/d$, and since one has $\nu > 1$ ford $d \leq 4$, one may conclude that the membrane is flat for $d \leq d_c = 4$. Since we cannot determine the accuracy of the Gaussian approximation, this estimate must be viewed largely as interesting speculation.
We have seen that numerical simulations provide good support for analytic results in the case of phantom membranes. When self-avoidance is included, numerical simulations become invaluable, since analytic results are harder to come by. Early simulations provided a first estimate of the size exponent at $d = 3$ fully compatible with the Flory estimate. The lattices examined were not very large, however, and subsequent simulations with larger volumes found that the $d = 3$ membrane is

actually flat. A different approach to weakening the flat phase, bond dilution, found that the flat phase persists until the percolation critical point. In conclusion the bulk of accumulated evidence indicates that flatness is an intrinsic consequence of self-avoidance. If this is indeed correct the SAFP coincides with FLFP and this feature is an inherent consequence of self-avoidance.
Given the difficulties of finding a crumpled phase with a repulsive potential, simulations for larger values of the embedding space dimension d have also been performed. These simulations show clear evidence that the membrane remains flat for $d = 3$ and 4 and undergoes a crumpling transition for $d \geq 5$, implying $d_c \geq 4$.
The enormous efforts dedicated to study the SAFP have not resulted in a complete clarification of the overall scenario since the existing analytical tools do not provide a clear picture. Numerical results clearly provide the best insight. For the physically relevant case $d = 3$, the most plausible situation is that there is no crumpled phase and that the flat phase is identical to the flat phase of the phantom model. For example, the roughness exponents ζ_{SA} from numerical simulations of self-avoidance at $d = 3$ and the roughness exponent at the FLFP compare extremely well,

$$\zeta_{SA} = 0.64(4), \quad \zeta = 0.64(2). \tag{15}$$

So the numerical evidence allows us to conjecture that the SAFP is exactly the same as the FLFP, and that the crumpled self-avoiding phase is absent in the presence of purely repulsive potentials (see Fig.6).

4 Anisotropic Membranes

An anisotropic membrane is a crystalline membrane having the property that the elastic or the bending rigidity properties in one distinguished direction are different from those in the $D - 1$ remaining directions. What this leads to is the generation of a completely new phase, in which the membrane is crumpled in some internal directions but flat in the remaining ones. A phase of this type is called a *tubular phase* and does not appear when studying isotropic membranes. So here, the phase diagram contains a crumpled, tubular and flat phase. The crumpled and flat phases are equivalent to the isotropic ones, so anisotropy turns out to be an irrelevant interaction in those phases. The new physics is contained in the tubular phase, which we describe briefly now.

4.1 The tubular phase

Since the physically relevant case for membranes is $D = 2$ we concentrate on the properties of the y-tubular phase. The key critical exponents characterizing the tubular phase are the size exponent ν, giving the scaling of the tubular diameter R_g with the extended L_y and transverse $L_\perp$ sizes of the membrane, and the roughness

exponent ζ associated with the growth of height fluctuations h_{rms}:

$$R_g(L_\perp, L_y) \propto L_\perp^\nu S_R(L_y/L_\perp^z) \tag{16}$$

$$h_rms(L_\perp, L_y) \propto L_y^\zeta S_h(L_y/L_\perp^z)$$

Here S_R and S_h are scaling functions and z is the anisotropy exponent. One can prove that there are some general scaling relations among the critical exponents. All three exponents may be expressed in terms of a single exponent:

$$\zeta = \frac{3}{2} + \frac{1-D}{2z} \tag{17}$$

$$\nu = \zeta z$$

The phantom case can be solved exactly. The result for the size exponent is

$$\nu_{Phantom}(D) = \frac{5-2D}{4} \rightarrow \nu_{Phantom}(2) = \frac{1}{4} \tag{18}$$

with the other exponents following from the scaling relations above.
The self-avoiding case may be treated with techniques similar to those in the isotropic case. For example, in a Flory approximation, one obtains

$$\nu_{Flory} = \frac{D+1}{d+1}. \tag{19}$$

5 The Crystalline-Fluid Transition and Fluid Membranes

A flat crystal melts into a liquid when the temperature is increased. This transition may be driven by the sequential liberation of defects. With increasing temperature, a crystal melts first to an intermediate hexatic phase via a continuous transition, and finally goes to a conventional isotropic fluid phase via another continuous transition. Two main points are worth keeping in mind when studying the more difficult case of fluctuating geometries. 1) The experimental evidence for the existence of the hexatic phase is not completely settled in those transitions which are continuous. 2) Some 2D crystals (like Xenon absorbed on graphite) melt to a fluid phase via a first order transition without any intermediate hexatic phase.
The straight-forward translation of the previous results to the tethered membrane would suggest a similar scenario. There would then be a crystalline to hexatic transition and a hexatic to fluid transition. Although the previous scenario is plausible, there are no solid experimental or theoretical results that establish it.
The Kosterlitz-Thouless argument shows that defects will necessarily drive a 2D crystal to melt. The entropy of a dislocation grows logarithmically with the system size, so for sufficiently high temperature, entropy will dominate over the dislocation

energy and the crystal will necessarily melt. If the same argument is applied now to a tethered membrane, the entropy is still growing logarithmically with the system size, while the energy becomes independent of the system size, so any finite temperature drive the crystal to melt, and the low temperature phase of a tethered membrane will necessarily be a fluid phase, either hexatic or a conventional fluid if a first order transition takes place. This problem has been investigated in numerical simulations, which provide some concrete evidence in favor of the hexatic phase scenario, although the issue is far from being settled.
The hexatic membrane is a fluid membrane that, in contrast to a conventional fluid, preserves the orientational order of the original lattice.

6 Conclusions

In this paper we have described the distinct universality classes of membranes with particular emphasis on crystalline membranes. We have presented qualitative and descriptive aspects of the physics with some technical results . We have shown that the phase diagram of the phantom crystalline membrane class is theoretically very well understood both by analytical and numerical treatments. To complete the picture it would be extremely valuable to find experimental realizations for this particular system. An exciting possibility is a system of cross-linked DNA chains together with restriction enzymes that catalyze cutting and rejoining. The difficult chemistry involved in these experiments is not yet under control, but it is hoped that these technical problems will be overcome in the near future.
There are several experimental realizations of self-avoiding polymerized membranes discussed in the text. The experimental results compare very well with the theoretical estimates from numerical simulations. As a future theoretical challenge, analytical tools need to be sharpened since they fail to provide a clear and unified picture of the phase diagram. On the experimental side, there are promising experimental realizations of tethered membranes which will allow more precise results than those presently available. Among them there is the possibility of very well controlled synthesis of DNA networks to form physical realizations of tethered membranes.
The case of anisotropic polymerized membranes has also been mentioned. The phase diagram contains a new tubular phase which may be realized in nature. There is some controversy about the precise phase diagram of the model, but definite predictions for the critical exponents and other quantities exist. Anisotropic membranes are also experimentally relevant. They may be created in the laboratory by polymerizing a fluid membrane in the presence of an external electric field.
Probably the most challenging problem, both theoretically and experimentally, is a complete study of the role of defects in polymerized membranes. There are a large number of unanswered questions, which include the existence of hexatic phases, the properties of defects on curved surfaces and its relevance to the possible existence of more complex phases. This problem is now under intense experimental investi-

gation.
Lastly, crystalline membranes also provide important insight into the fluid case, since any crystalline membrane eventually becomes fluid at high temperature. Due to its relevance in many physical and biological systems and its potential applications in material science, the experimental and theoretical understanding of fluid membranes is one of the most active areas in soft condensed matter physics.

References

[1] M. J. Bowick, A. Travesset, *The statistical mechanics of membranes* (preprint), to appear in Physics Reports in the proceedings of RG2000, Taxco, 1999.

[2] P. M. Chaikin, T. C. Lubensky, *Principles of Condensed Matter Physics*, Cambridge Univ. Press, 1995.

[3] G. Gompert, D. M. Kroll, *Network models of fluid, hexatic and polymerized membranes*, J. Phys: Cond. Mat. **9**(1997)

[4] D. Nelson, T. Piran, S. Weinberg, eds., *Statistical Mechanics of Membranes and Surfaces*, vol.5, World Scientific, 1989.

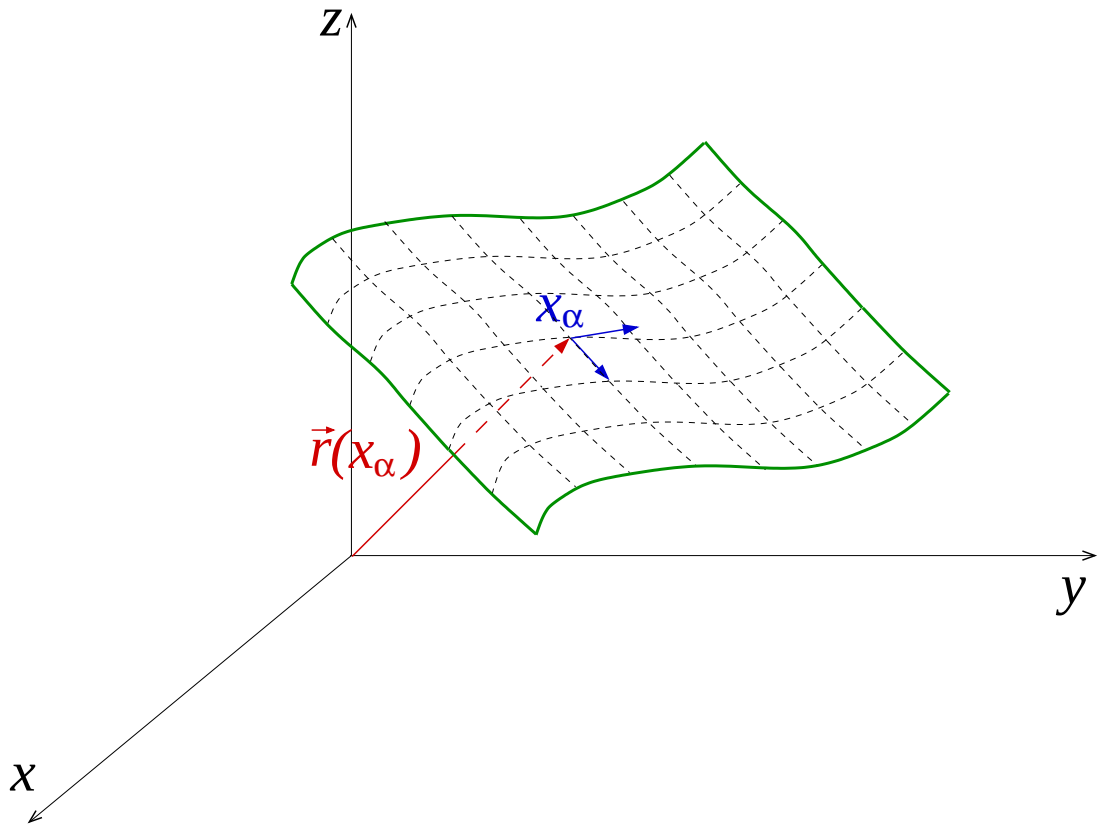

Figure 1: Representation of a membrane.

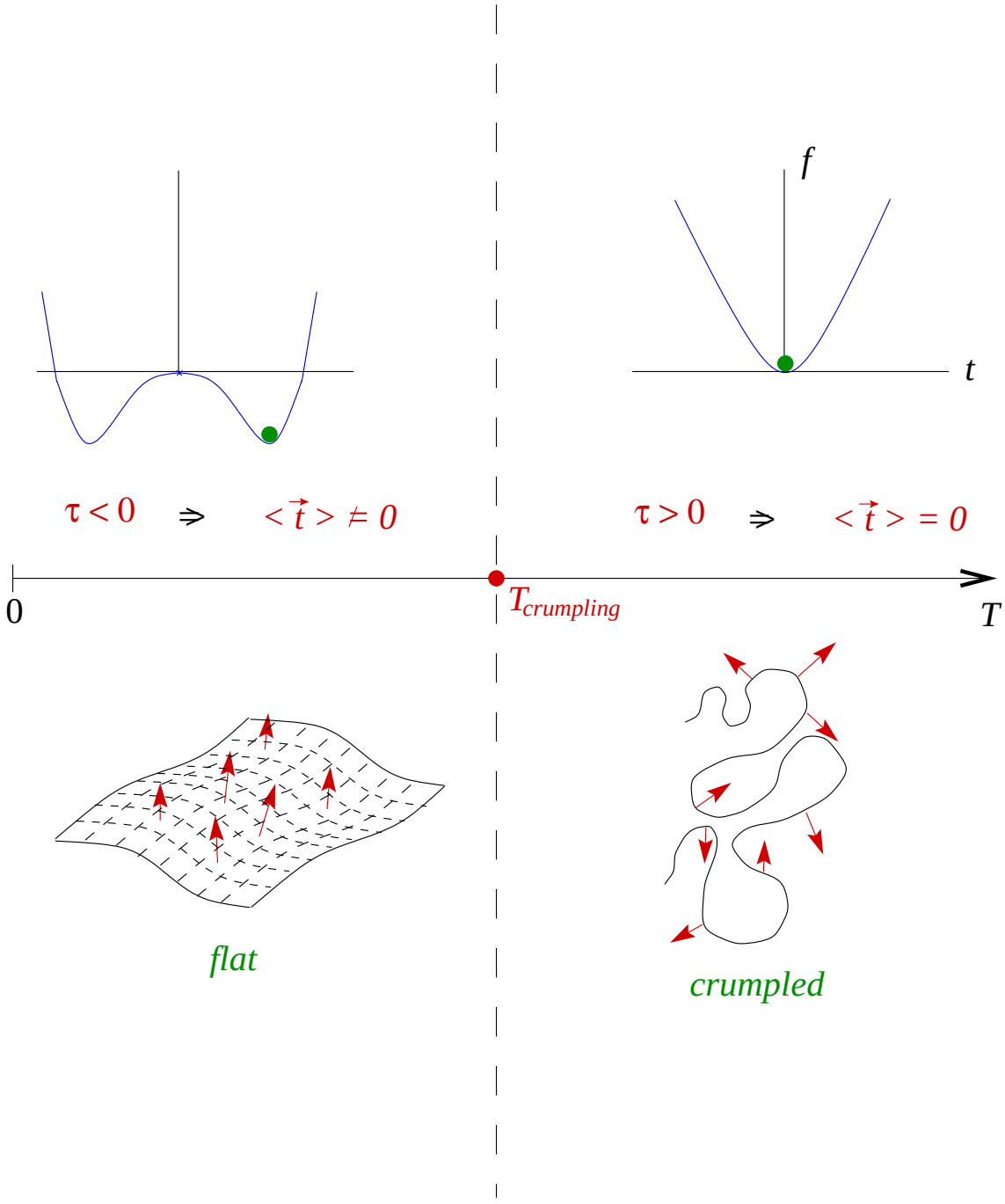

Figure 2: Mean field solutions for crystalline membranes.

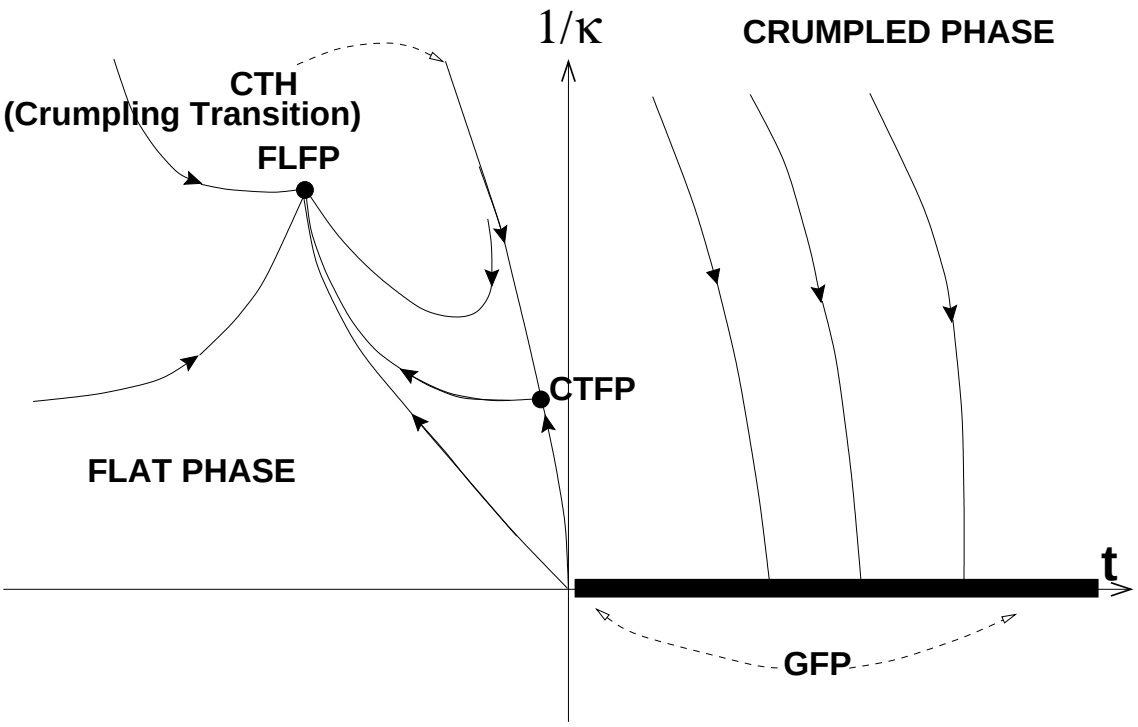

Figure 3: Phase diagram for phantom membranes.

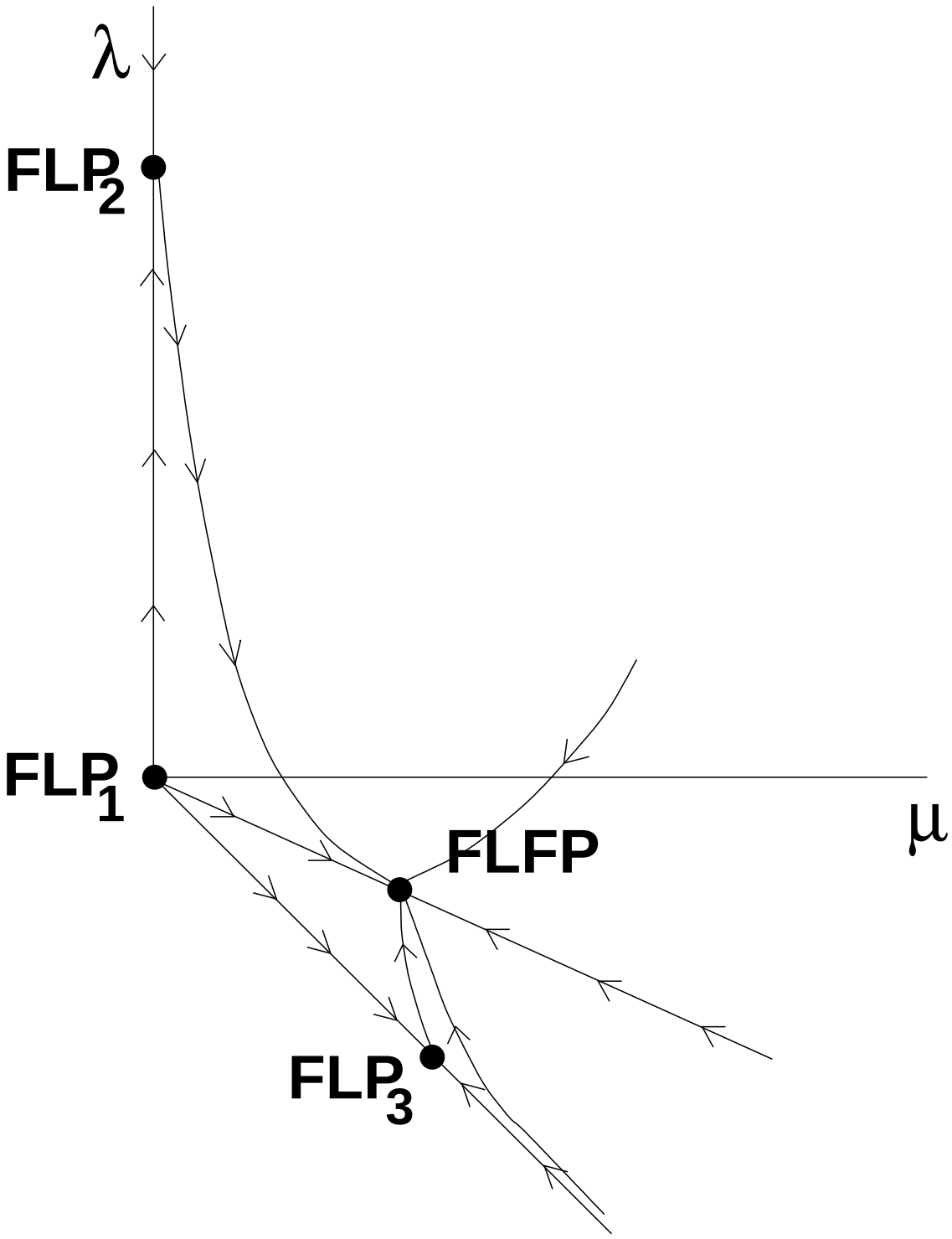

Figure 4: Phase diagram for the phantom flat phase.

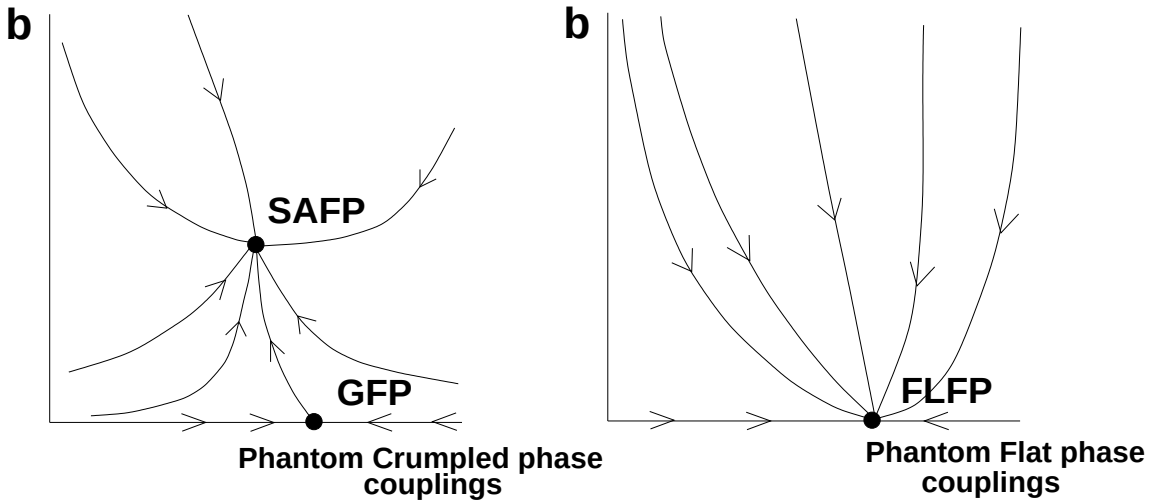

Figure 5: The addition of self-avoidance at the crumpled and flat phases.

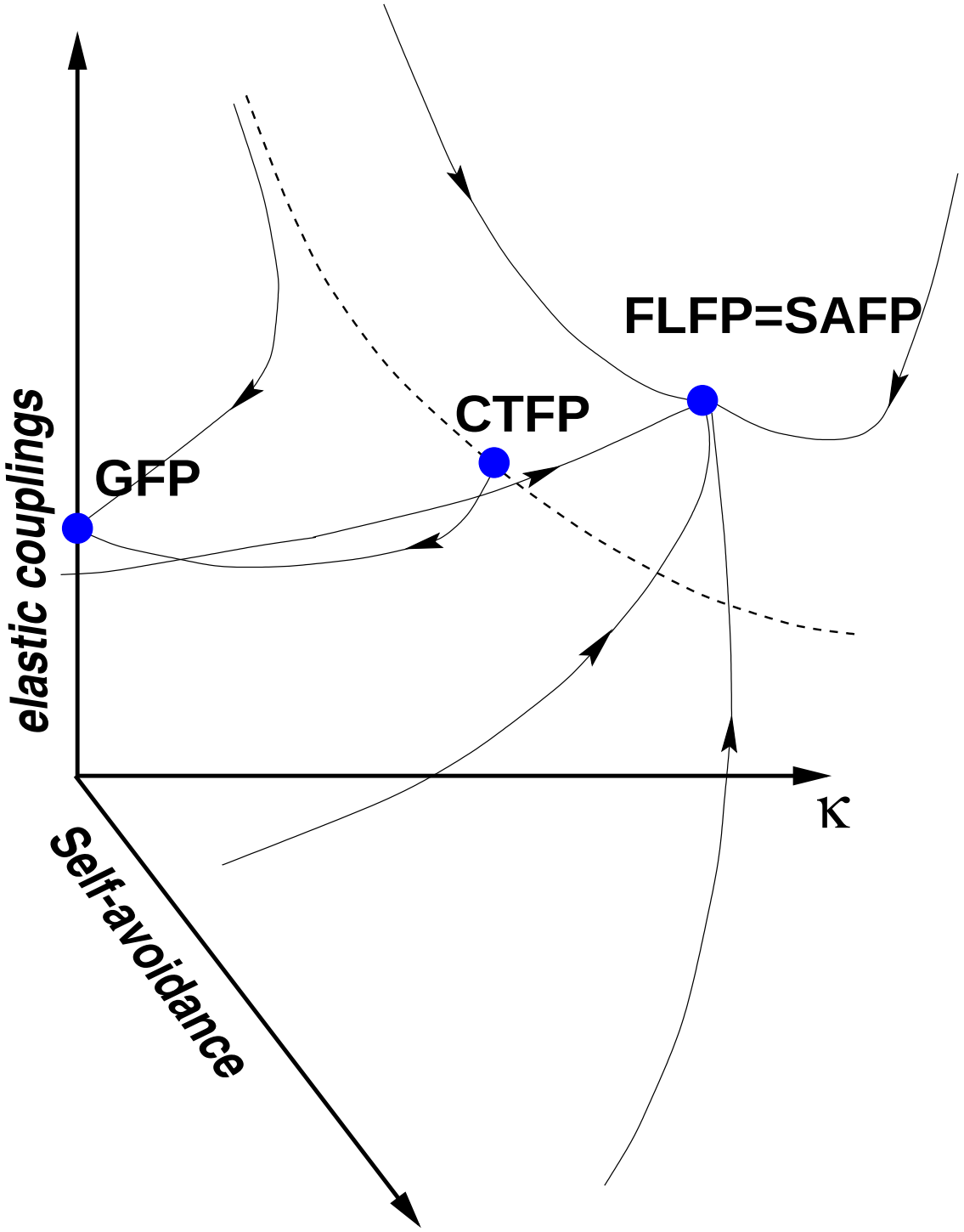

Figure 6: The conjectured phase diagram for the self-avoiding crystalline membrane in d=3. With any degree of self avoidance, the flows are to the flat fixed point of the phantom model(FLFP).